

WAVELET BASED WATERMARKING ON 3D IRREGULAR MESHES

M. Hachani, A. Ouled zaid

National Engineering School of Tunis
Communication Systems Laboratory
B.P. 37 le Belvédère 1002 Tunis, Tunisia

ABSTRACT

This paper proposes a blind and high-capacity watermarking framework for 3D triangle meshes. The basic idea is to use a quantization based approach in the transform domain to embed the secret message. Our proposal can be applied to regular as well as irregular meshes by using irregular wavelet-based analysis. The watermark is inserted in an appropriate resolution level by quantizing the norms of wavelet coefficients vectors. Simulation results show that our watermarking framework is robust to common geometric attacks and can provide relative high data embedding rate whereas keep a relative lower distortion.

Index Terms— Information security, Watermarking, Discrete wavelet transforms, Quantization, Image decomposition

1. INTRODUCTION

In the last decade, with the interest and requirement of 3D models in industrial, medical and entertainment applications, 3D mesh watermarking has received much attention in the community [1, 2]. Specifically, high-capacity (H-C) mesh watermarks are sometimes very useful to carry a large amount of auxiliary information, such as the mesh generation information, a description, a related website address, or even animation parameters. The existing mesh watermarking algorithms can fall into two broad categories: spatial domain methods and frequency-domain methods. The most favorable of them are frequency-domain algorithms since they provide better robustness and imperceptibility. Besides the direct mesh spectral domain, a watermark can also be embedded in the multiresolution domain. In the case of 3D meshes, multiresolution analysis seems more flexible than the other spectral-like transforms, in sense that it provides different embedding locations that can satisfy different application requirements. Moreover, the mesh multiresolution analysis based on wavelet transform is a very suitable tool for constructing an imperceptible and high-capacity watermarking system. Based on the regular wavelet analysis, Kanai *et al.* [3], proposed a non-blind watermarking algorithm for 3D meshes. Uccheddu *et al.* [4] extends [3] to achieve a blind watermark detection. Recently, Wang *et al.* [5] developed

a hierarchical watermarking framework based on wavelet transform of the semiregular meshes. The aforementioned wavelet based watermarking schemes cannot process irregular meshes directly. They can embed the watermark into an irregular mesh by using remeshing that converts an irregular mesh into a semi-regular one. But, the remeshed model cannot be seen as identical to the original, as it corresponds to a different sampling of the underlying 3D surface. Consequently, the watermark robustness and imperceptibility may be degraded due to this remeshing preprocessing. Using the direct irregular mesh wavelet analysis tool [6], Kim *et al.* [7] proposed a similar correlation-based scheme as in [4] to embed watermark components in bins (groups) of WCVs. Despite its robustness against various geometric attacks, Kim *et al.* method is penalized by its limited payload capacity and quality degradation.

In the present work, we propose a 3D mesh watermarking method which can be used in data hiding applications. The motivation is to design a blind watermarking system, taking into account the capacity-imperceptibility-robustness-simplicity requirements. For this purpose, we employ an alternative to Quantization Index Modulation (QIM) approach [8] to embed the secret message in the wavelet transform domain. Our proposal can be applied to irregular as well as regular meshes by using irregular lifting-based wavelet analysis introduced by Valette [6]. The selected watermarking primitive is the norms of the wavelet coefficient vectors (WCVs), at a certain appropriate resolution level. This primitive is invariant to similarity transformations which include translation, rotation and uniform scaling. Experimental results show that despite its simplicity, our approach is characterized by large payloads, robustness to several attack scenarios, and high visual quality reconstruction.

The rest of this paper is organized as follows. In Section 2, we explain our watermarking approach in detail. In Section 3, we show some of our experimental results. Finally, in Section 4, we conclude and mention potential improvement in future work.

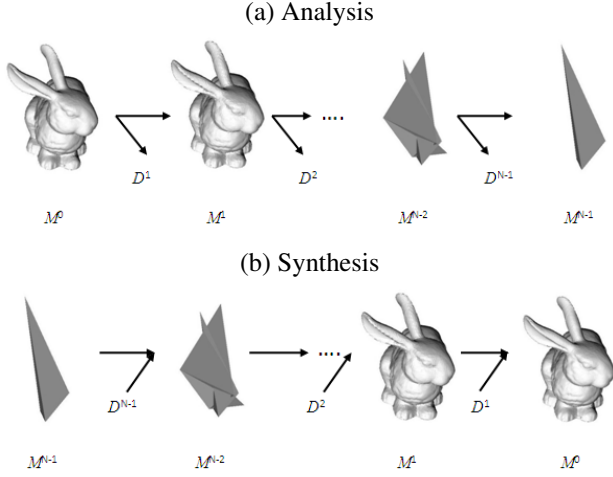


Fig. 1. Construction of multiresolution mesh, (a) analysis, (b) synthesis.

2. PRESENTATION OF THE PROPOSED WATERMARKING FRAMEWORK

The watermark embedding space in our system is the wavelet transform domain. We choose to embed the watermark by quantizing the norms of the WCVs associated with a specific multiresolution level. After applying the Discrete Wavelet Transform (DWT) on the cover irregular mesh, the watermark message is embedded using non-linear scaling QIM (NLS-QIM) watermark design. It is worth mentioning that QIM method is a widely used quantization-based embedding technique for image, audio and video watermarking. Its popularity is, in part, due to its ease of implementation, computational flexibility and large data payloads.

2.1. Multiresolution analysis

Recent works showed that the 3D mesh multiresolution approach provides very efficient watermarking methods. Such an analysis produces a coarse mesh that represents the basic shape (low frequencies) of the model and a set of details information at different resolution levels (medium and high frequencies). During the dual synthesis process, we can obtain a series of reconstructed meshes, all representing the same 3D model but with different resolution levels.

Here, we briefly recall the principle of the multiresolution analysis (performed by a 3D Discrete Wavelet Transform) of irregular meshes, which is proposed by Valette and Prost [6]. First, a mesh M^0 is simplified according to an inverse irregular subdivision scheme where each face can be subdivided into four, three, or two faces, or remain unchanged. After the simplification is complete, one can build a hierarchical relationship between the original mesh M^0 and the simplified one. Therefore, at a given decomposition level, j , the ge-

ometry of M^j can be approximated by applying the wavelet decomposition, with two analysis filters. Figures 1a and 1b illustrate the analysis and the synthesis principles respectively. In our work, we used a lifting implementation of the analysis and synthesis filter-banks. The aforementioned process is performed iteratively to finally obtain the coarsest-level irregular mesh M^J and sets of WCVs. By using irregular wavelet analysis scheme, our watermarking method can be applied for both regular and irregular 3D meshes.

2.2. Watermark embedding stage

In our watermark embedding approach, we only consider the set $D^j = [d_0, d_1, \dots, d_{N-1}]^t$ of WCVs associated with the j^{th} intermediate wavelet decomposition level. The Cartesian coordinates of the coefficients $d_i, i \in \{0, \dots, N-1\}$ are converted to spherical coordinates $[r_i, \theta_i, \phi_i]^t$ where, $r_i = \|d_i\|$ denotes norm of wavelet coefficient vector d_i . Let us consider the watermark message as a binary sequence assigned by $m = \{m_0, \dots, m_i, \dots, m_{N-1}\}$, with $m_i \in \{0, 1\}$. These bits are inserted by quantifying the WCV norms r_i according to $\tilde{r}_i = \lfloor \frac{r_i}{\Delta} \rfloor \times \Delta$. The binary decision results on two watermarked components c_0 and c_1 depending on the quantizer value Δ and the scaling parameter α . When $b_i = 0$ is considered, the binary decision results on the watermarked component c_0 , given by:

$$\begin{aligned} \text{if } r_i \in [\tilde{r}_i + \alpha, \tilde{r}_i + \frac{\Delta}{2} - \alpha] &\rightarrow c_0 = r_i; \\ \text{if } r_i \in [\tilde{r}_i, \tilde{r}_i + \alpha] &\rightarrow c_0 = \tilde{r}_i + \alpha; \\ \text{if } r_i > \tilde{r}_i + \frac{\Delta}{2} - \alpha &\rightarrow c_0 = \tilde{r}_i + \frac{\Delta}{2} - \alpha; \end{aligned} \quad (1)$$

Otherwise, if $b_i = 1$ is considered, c_1 is given by:

$$\begin{aligned} \text{if } r_i \in [\tilde{r}_i + \frac{\Delta}{2}, \tilde{r}_i + \frac{\Delta}{2} + \alpha] &\rightarrow c_1 = \tilde{r}_i + \frac{\Delta}{2} + \alpha; \\ \text{if } r_i \in [\tilde{r}_i + \frac{\Delta}{2} + \alpha, \tilde{r}_i + \Delta - \alpha] &\rightarrow c_1 = r_i; \\ \text{if } r_i > \tilde{r}_i + \Delta - \alpha &\rightarrow c_1 = \tilde{r}_i + \Delta - \alpha; \end{aligned} \quad (2)$$

This results in the watermarked component r'_i , that yields maximum correlation with r_i for a given scaling parameter α .

2.3. Watermark recovery stage

A given reconstructed WCV norm r'_i , positioned in the j^{th} decomposition level, is manipulated using Equation 3 to obtain Q^0 and Q^1 indices.

$$\begin{aligned} Q^0 &= \begin{cases} \lfloor \frac{r'_i}{\Delta} \rfloor & \text{if } r'_i \geq 0 \\ \lfloor \frac{-r'_i}{\Delta} \rfloor & \text{otherwise} \end{cases} \\ Q^1 &= \begin{cases} \lfloor \frac{r'_i + \frac{\Delta}{2}}{\Delta} \rfloor & \text{if } r'_i \geq 0 \\ \lfloor \frac{-r'_i - \frac{\Delta}{2}}{\Delta} \rfloor & \text{otherwise} \end{cases} \end{aligned} \quad (3)$$

At this step, we measure the distance between r'_i and its approximation, as follows:

$$\begin{aligned} \text{if } |r'_i - (Q^1 \times \Delta)| < |r'_i - (Q^0 \times \Delta)| &\rightarrow m_i = 1 \\ \text{else} &\rightarrow m_i = 0 \end{aligned} \quad (4)$$

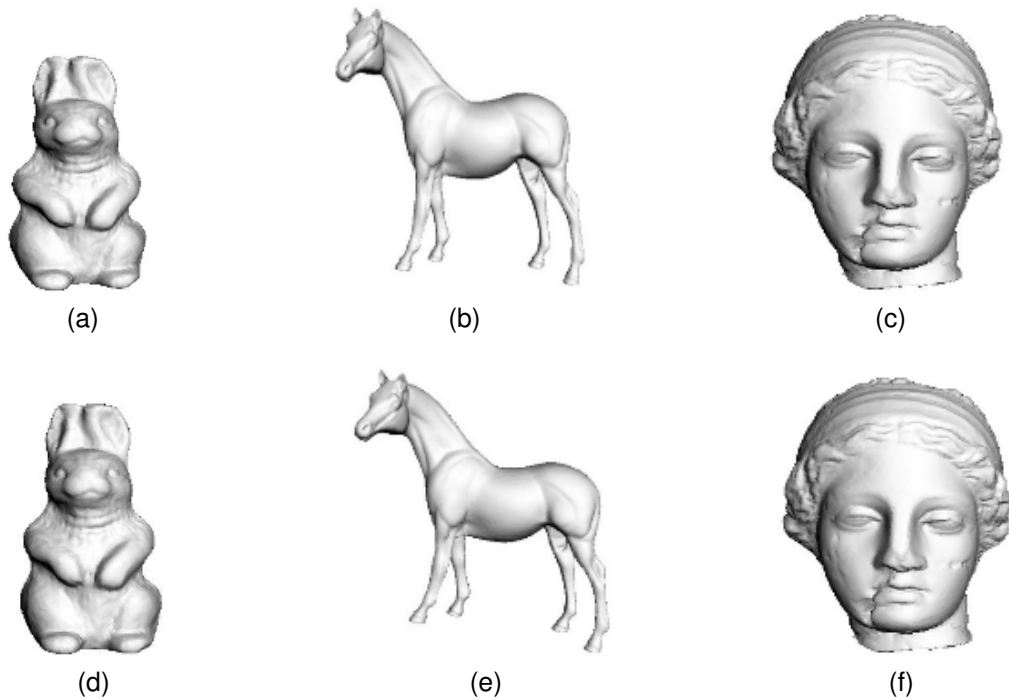


Fig. 2. The watermarked irregular meshes (a) Rabbit, (b) Horse, and (c) Venus. The corresponding nonwatermarked meshes are also provided as (d)-(f) for comparison.

The capacity of our watermarking approach is equal to the number of wavelet coefficients N in the considered resolution level. In our experiments, the embedding level (EL) corresponds to the third resolution level ($j = 3$).

3. EXPERIMENTAL RESULTS

We have tested our high-capacity watermarking algorithm on several irregular meshes: Venus (100759 vertices), Rabbit (70658 vertices), Horse (112642 vertices), Bunny (34835 vertices), Davidhead (23889 vertices), and Hand (36619 vertices). Concerning the parameter setting, for the QIM based embedding, the quantizer step size Δ and the α parameter are fixed at 8 and 0.2 respectively, which appear to provide good performances for most of the models. The embedding process was performed on the norms of WCVs at the third resolution level (EL=3). Quality assessment was carried out using two evaluation criteria, maximum root mean square error (MRMS), and mesh structural distortion measure (MSDM). MRMS measures the objective distortion between watermarked and original meshes. A perceptual distance between them is assessed by the MSDM. The robustness is evaluated by the normalized correlation [9] ($corr$) between the extracted watermark binary message and the originally embedded one.

3.1. Basic Simulations

Tables 1 and 2 illustrate the baseline evaluations of the proposed H-C watermarking framework. From the results reported in these tables, it can be seen that, for all the tested meshes, our method introduces relatively high-amplitude deformation while keeping it imperceptible (the induced MSDM is less than 0.078). This point is also confirmed in Figure 2, where three original and watermarked meshes are depicted. We can hardly observe any visual difference between the cover and watermarked models. In practice, perceptual distortion measurement is considered more important than the objective distortion measurement since it does not always correctly reflect the visual difference between two meshes. It is worthwhile pointing out that mesh-based applications have very different restrictions on the objective and perceptual distortions induced by the watermark embedding. For example, for the meshes used in digital entertainment, we should ensure that the induced distortion is not annoying to human eyes, while the amount of induced objective distortion is less important. On the other hand, in some mesh applications, such as computer-aided design and medical imaging, it is often required that the induced objective distortion should be very small, while the visual quality of the watermarked model is relatively less important.

The results reported in Tables 1 and 2 also compares the capacity, the watermark correlation ($corr$), and the MRMS

Table 1. Baseline evaluations of the proposed watermarking framework and Wang’s methods for Venus, Rabbit and Horse meshes (in the parentheses are the results of Wang *et al* H-C watermarking method [5]).

| | Venus | Rabbit | Horse |
|--------------------|----------------|---------------|--------------|
| EL | 3 (4) | 3 (4) | 3 (4) |
| Payload (kbits) | 10.909 (7.632) | 3.312(3.18) | 5.28(5.247) |
| MRMS (10^{-3}) | 0.2 (0.22) | 0.38 (0.2) | 0.4(0.15) |
| MSDM | 0.04 (0.045) | 0.021 (0.039) | 0.038(0.058) |
| <i>corr</i> | 1 (1) | 1 (1) | 1 (1) |

Table 2. Baseline evaluations of the proposed watermarking framework and Kim’s methods for Bunny, Hand and David head meshes (in the parentheses are the results of Kim *et al* method [7]).

| | Bunny | Hand | David head |
|--------------------|---------------|-------------|--------------|
| EL | 3 (1) | 3 (1) | 3 (1) |
| Payload (kbits) | 2.986 (0.265) | 3.26(0.265) | 1.374(0.265) |
| MRMS (10^{-3}) | 0.3 (7) | 0.5(9) | 1.4(24) |
| MSDM | 0.024 | 0.045 | 0.078 |
| <i>corr</i> | 1 (1) | 1 (1) | 1 (1) |

measures provides by our method with those provided by two existing wavelet-based high-capacity methods (without any robustness consideration): Wang *et al* method [5] (for Venus, Rabbit, Horse meshes), and Kim *et al* method [7] (for Bunny, Davidhead, and Hand meshes). It should be noted that in the case of Wang *et al* watermarking algorithm, the tested mesh is first remeshed to construct a semi-regular mesh before passing through the wavelet decomposition process.

3.2. Watermark robustness under geometric attacks

In this section, we propose to assess the resistance of the embedded watermark under various geometric attacks, including noise addition, smoothing, and lossy compression. Tables 3, 4 and 5 presents the robustness evaluation results in terms of the normalized correlation *corr*. The distortion induced by attacks is also measured by MRMS and MSDM. The results of the robust watermarking method in [10], based on manifold harmonics transform, are presented in parentheses. It can be seen that with a roughly comparable robustness level, Wang *et al* [10] embedding technique introduces higher geometric and perceptual distortions than our method. Additionally, the watermark message length is relatively short, of about 64 bits, which is still negligible compared to our watermarking approaches capacity. Hence, we can assume that our watermark-

Table 3. Robustness against the random noise addition (in the parentheses are the results of Wang *et al* Robust watermarking method [10]).

| Model | Noise | <i>corr</i> | MSDM |
|--------|--------|-------------|--------------|
| Venus | 0.05 % | 0.99 (0.85) | 0.097 (0.28) |
| | 0.25 % | 0.99 (0.59) | 0.108 (0.7) |
| | 0.5 % | 0.99 (0.31) | 0.119 (0.83) |
| Rabbit | 0.05 % | 0.99 (0.92) | 0.099 (0.18) |
| | 0.25 % | 0.99 (0.59) | 0.105 (0.6) |
| | 0.5 % | 0.99 (0.31) | 0.111 (0.77) |
| Horse | 0.05 % | 0.99 (0.69) | 0.105 (0.23) |
| | 0.25 % | 0.99 (0.5) | 0.114 (0.64) |
| | 0.5 % | 0.98 (0.08) | 0.12 (0.78) |

Table 4. Robustness against the Laplacian smoothing in the parentheses are the results of Wang *et al* Robust watermarking method [10]).

| Model | Iterations | <i>corr</i> | MSDM |
|--------|------------|-------------|--------------|
| Venus | 10 | 0.99 (0.74) | 0.101 (0.15) |
| | 30 | 0.99 (0.71) | 0.117 (0.27) |
| | 50 | 0.98 (0.62) | 0.135 (0.34) |
| Rabbit | 10 | 0.99 (0.90) | 0.08 (0.15) |
| | 30 | 0.99 (0.71) | 0.11 (0.26) |
| | 50 | 0.99 (0.45) | 0.142 (0.31) |
| Horse | 10 | 0.99 (0.97) | 0.092 (0.15) |
| | 30 | 0.99 (0.5) | 0.102 (0.23) |
| | 50 | 0.99 (0.35) | 0.135 (0.28) |

ing scheme has a better trade-off between the robustness, the induced distortion and the capacity payload. However, due to the synchronization issue caused from the wavelet approach of 3-D irregular meshes, we do not consider the resistance under connectivity attacks.

4. CONCLUSION

In this paper, we have reported a new high-capacity watermarking framework for irregular meshes. Our watermarking framework consists on QIM based embedding approach applied to the norms of wavelet coefficient vectors. Preliminary experimental investigations demonstrate important embedding payloads with the respect to the subjective/objective watermarked mesh quality. The experimental results also in-

Table 5. Robustness against coordinate quantization (in the parentheses are the results of Wang *et al* Robust watermarking method [10]).

| Model | Quantization | <i>corr</i> | MSDM |
|--------|--------------|-------------|-------------|
| Venus | 9-bits | 0.99 (0.93) | 0.12 (0.49) |
| | 8-bits | 0.98 (0.70) | 0.26 (0.66) |
| | 7-bits | 0.97 (0.63) | 0.42 (0.79) |
| Rabbit | 9-bits | 0.99 (0.84) | 0.09 (0.44) |
| | 8-bits | 0.99 (0.59) | 0.29 (0.61) |
| | 7-bits | 0.98 (0.05) | 0.53 (0.76) |
| Horse | 9-bits | 0.99 (0.61) | 0.11 (0.44) |
| | 8-bits | 0.97 (0.25) | 0.36 (0.60) |
| | 7-bits | 0.97 (0.17) | 0.51 (0.73) |

dicating that the watermark message exhibits a high robustness against various kinds of geometric attacks such as similarity transformation, lossy compression, gaussian noise and smoothing.

In our future work, we plan to apply a re-ordering process on the original model before irregular wavelet analysis to achieving the robustness against connectivity reordering attacks. Additionally, adaptive setting of the QIM parameters may lead to a better robustness and meanwhile a less induced perceptual distortion.

5. REFERENCES

- [1] K. Wang, G. Lavoué, F. Denis, and A. Baskurt, "A Comprehensive Survey on Three-Dimensional Mesh Watermarking," *IEEE Transactions on Multimedia*, vol. 10, no. 8, pp. 1513–1527, December 2008.
- [2] P. Rondao-Alface and B. B. Macq, "From 3d mesh data hiding to 3d shape blind and robust watermarking: A survey," *Lect. Notes Comput. Sci. Trans. Data Hiding Multimedia Security*, vol. 2, pp. 99–115, 2007.
- [3] S. Kanai, D. Date, and T. Kishinami, "Digital watermarking for 3d polygon using multiresolution wavelet decomposition," in *Sixth IFIP WG 5.2 GEO-6*, 1998, pp. 296–307.
- [4] F. Ucheddu, M. Corsini, and M. Barni, "Wavelet-based blind watermarking of 3d models," in *Workshop on Multimedia and security*, ACM Press, 2004, pp. 143–154.
- [5] K. Wang, G. Lavou, F. Denis, and A. Baskurt, "Hierarchical Watermarking of Semiregular Meshes Based on Wavelet Transform," *IEEE Transactions on Information Forensics and Security*, vol. 3, no. 4, pp. 620–634, December 2008.
- [6] S. Valette and R. Prost, "Multiresolution analysis of irregular surface meshes," *IEEE Transactions on Visualization and Computer Graphics*, vol. 10, pp. 113–122, 2004.
- [7] M.S. Kim, S. Valette, H.Y. Jung, and R. Prost, "Watermarking of 3D irregular meshes based on wavelet multiresolution analysis," in *International Workshop on Digital Watermarking (IWDW'05)*, 2005, pp. 313–324.
- [8] B. Chen and G. W. Wornell, "Quantization index modulation, a class of provably good methods for digital watermarking and information embedding," *IEEE Transactions on Information Theory*, vol. 47, no. 4, pp. 1423–1443, 2001.
- [9] I.J. Cox, M.L. Miller, J.A. Bloom, J. Fridrich, and T. Kalker, *Digital Watermarking and Steganography*, Morgan Kaufmann Publishers Inc., 2007.
- [10] K. Wang, M. Luo, A.G Bors, and F. Denis, "Blind and robust mesh watermarking using manifold harmonics," in *IEEE International Conference on Image Processing (ICIP)*, 2009, pp. 3657–3660.